The Abdus Salam
International Centre for Theoretical Physics

United Nations
Educational, Scientific
and Cultural Organization

International Atomic
Energy Agency

SMR. 1643?2

WINTER COLLEGE ON OPTICS ON OPTICS AND PHOTONICS IN NANOSCIENCE AND NANOTECHNOLOGY

(7 - 18 February 2005)

"*Microstructured Fibers*"

presented by:
V. Degiorgio
Dipartmento de Elettronica
Università di Pavia
Italy

Microstructured fibers

Vittorio Degiorgio
Dipartimento di Elettronica
Università di Pavia
Italy

Summary

- Limitations of standard optical fibers
- MFs: structure
- MFs: properties
- MFs: some applications (see also the seminar by Ilaria Cristiani)

MFs: glass fibers with microscopic air holes running parallel to fiber axis

- Photonic crystal fibers (Russell, University of Bath)
- Microstructured fibers (Eggleton and Windeler, Bell Labs)
- Holey fibers (Richardson et al., ORC Southampton)
- Recent book: A. Bjarklev, J. Broeng, and A. Sanchez Bjarklev "Photonic Crystal Fibers" Kluwer 2003

Limitations of Standard Fibers

- Single-mode over a limited wavelength range

$$= \frac{2\pi a}{\lambda}\sqrt{n_1^2 - n_2^2} \le 2.4$$

- Rather small single-mode area: limited propagating power because of nonlinearities
- Single-mode area is not small enough for the exploitation of nonlinear interactions: long fibers are required
- Limited possibility of modifying the group-velocity dispersion curve

λ_{ZD} > 1.3 μm in silica glass

- Limited control of birefringence

Standard fibers: dispersion

Electric field of the propagating mode: $E(x,y,z,t) = E_o A(x,y)\exp[i(\omega t-\beta z)]$

The propagation constant β depends on ω

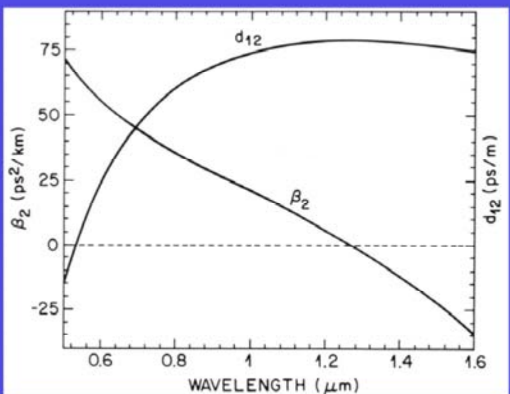

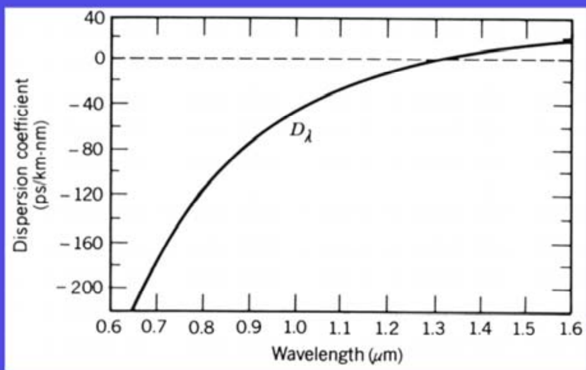

$$\beta_2 = \frac{\partial^2 \beta}{\partial \omega^2} \cong \frac{\omega}{c}\frac{\partial^2 n}{\partial \omega^2}$$

$$D = \frac{\partial \beta_1}{\partial \lambda} = -\frac{2\pi c}{\lambda}\beta_2$$

Pulse duration: $\Delta t = \Delta t_o \sqrt{1 + \left(z / z_L\right)^2}$ where: $z_L = \frac{\Delta t_o^2}{\beta_2}$

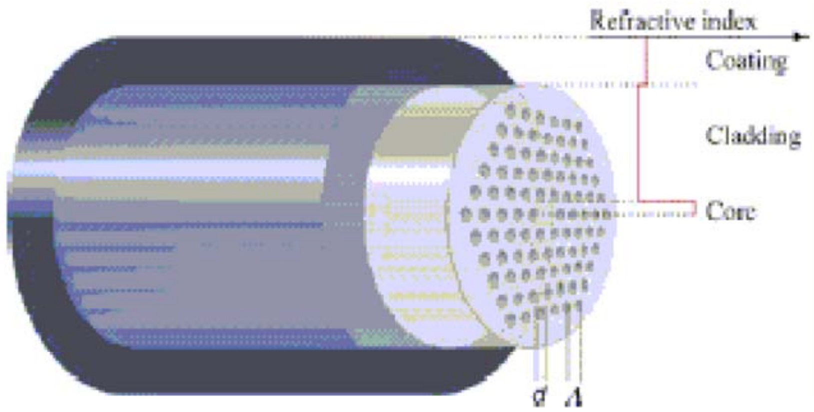

Figure 2 Schematic of the classical triangular cladding single-core photonic crystal fiber in which light is guided in a solid core embedded in a triangular lattice of air holes. The fiber structure is determined by the hole-size, d, and the hole-pitch, Λ. Like standard fibers, the PCF is coated with a high index polymer for protection and to strip off cladding-modes.

Crystal-Fibre Report

PCF with silica core

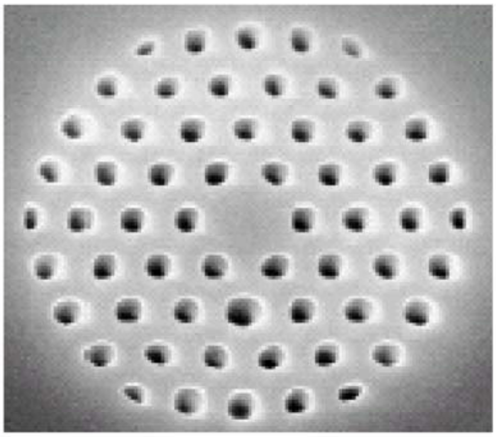

Figure 2 (b). A PCF in which light is guided in a silica core by an array of air holes of intermediate size, causing just a single mode to be guided independent of the wavelength of excitation or the scale of the structure.

PCF with air core

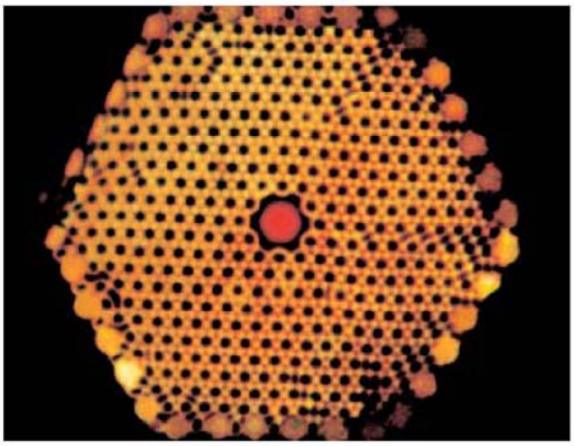

Figure 4. Optical micrograph showing the output face of an air-core fiber when the input is illuminated with a white-light source. Bright red light in the large central hole is trapped by the bandgap of the periodic cladding; other colors have quickly leaked away.

Microstructured fibers

Fiber fabricated at ORC,
University of Southampton, UK

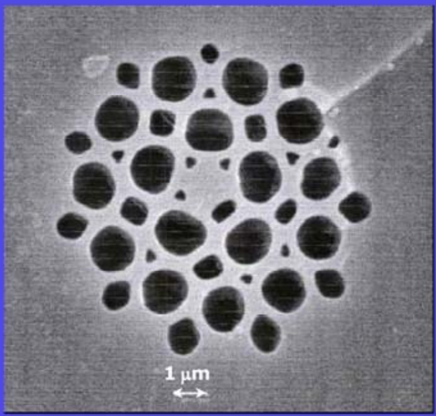

Photonic bandgap fiber

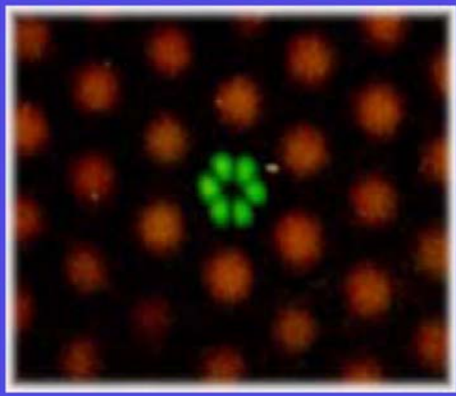

Any distribution of holes gives rise to a radially averaged refractive index that decreases as a function of the radius

Guided propagation inside a defect created in a periodic array of holes giving rise to a 2D photonic bandgap structure

PCF: fabrication

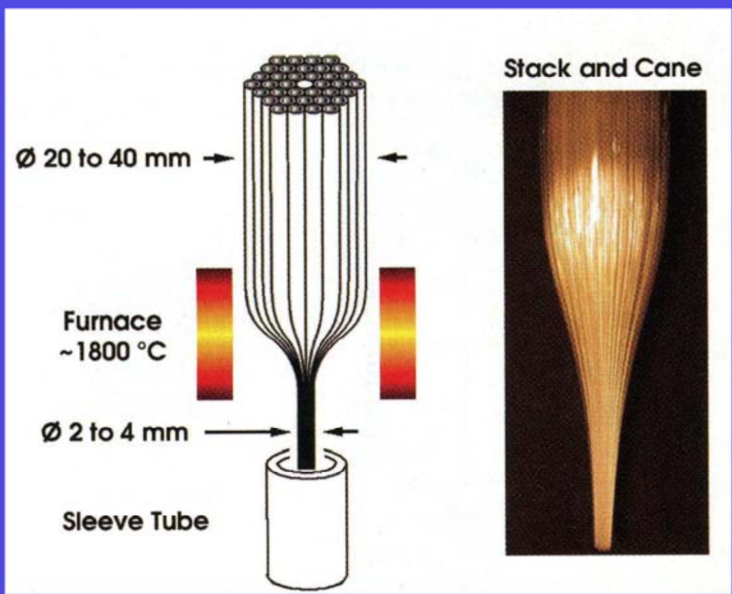

A bundle of silica capillaries is drawn down to a cane of a few mm in diameter. The cane is then inserted into a silica sleeve tube and drawn down again to a fiber of typically 125 μm in diameter. [H. Sabert and J. Knight, Photonics Spectra, August 2003]

Hollow-core Bragg fiber

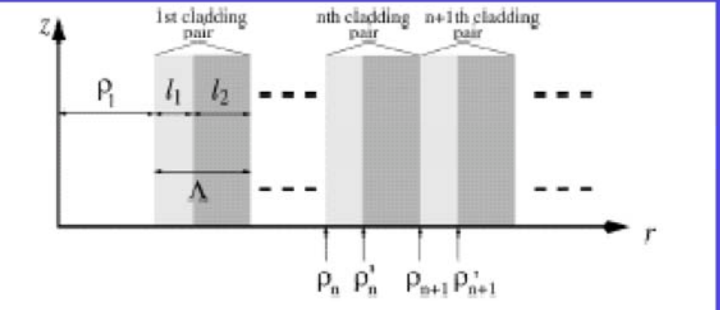

Fig. 1. Schematic of the $r-z$ cross section of a Bragg fiber. The fiber core has refractive index n_c and radius ρ_1. The fiber cladding is composed of pairs of alternating layers of high- and low-index material. The high-index layer has refractive index n_1 and thickness l_1. The low-index layer has refractive index n_2 and thickness l_2.

Fibers in which light confinement is due to cylindrical Bragg reflection instead of total internal reflection. Light guidance in an air-core is possible.

Properties and applications of silica-core PCFs

- Single-mode behavior over an extended wavelength range.

- Possibility to tailor fiber dispersion: dispersion compensation, pulse compression, control of soliton behavior, ...

- Possibility to tailor the effective area for the fundamental mode: very large area for transmitting powerful beams or very small area to enhance nonlinear properties.

- Control of birefringence

Single-mode condition

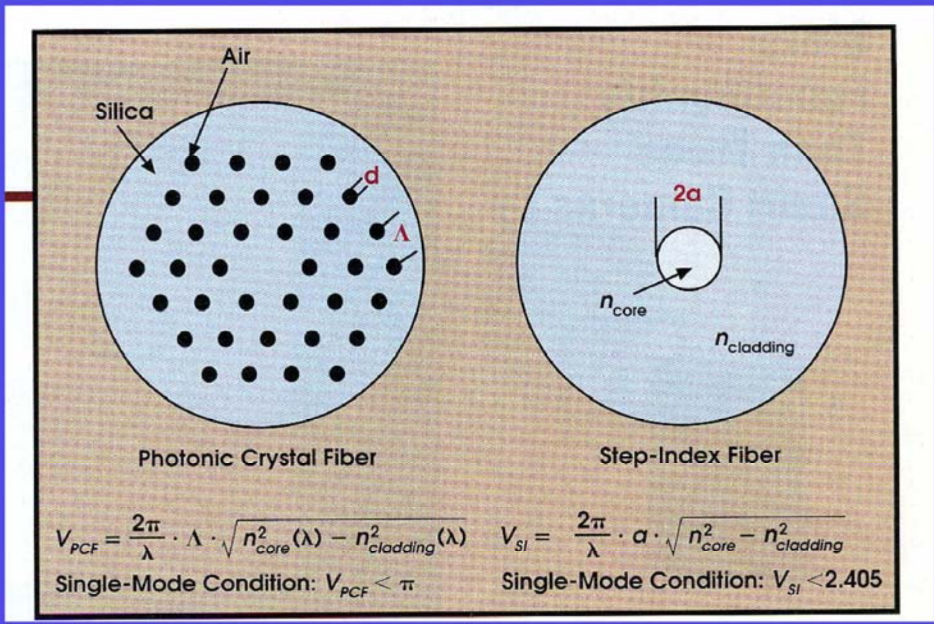

J. Limpert et al., Photonics Spectra, May 2004

N.A. Mortensen et al., Opt. Lett. 28, 1879 (2003)

Single-mode condition

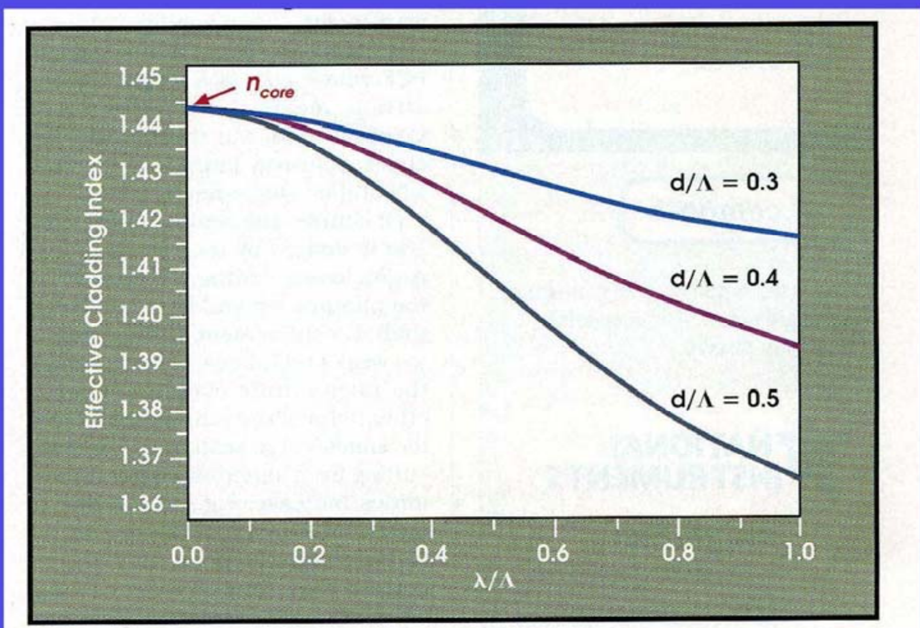

Figure 3. *The effective refractive index of a PCF's cladding has a very strong wavelength dependence.*

Single-mode condition

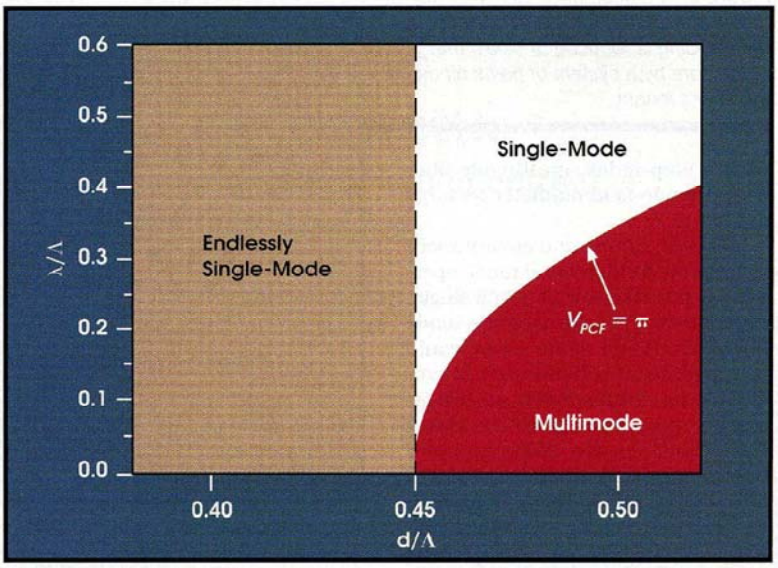

Figure 4. *If the holes in the cladding have a diameter-to-spacing ratio of less than 0.45, the fiber is "endlessly single-mode"; i.e., a single-mode fiber at any wavelength.*

PCF: group-velocity dispersion

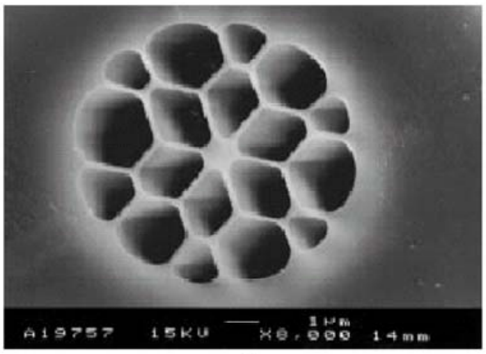

(a)

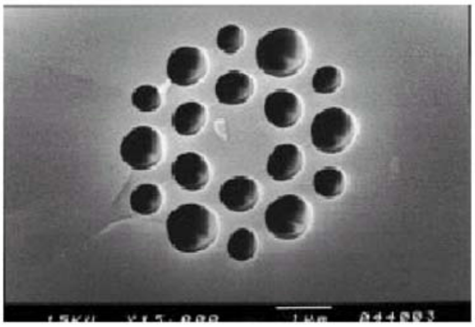

(b)

Scanning electron micrographs of the cleaved end-face of two PCFs.

a) Core diameter 1μm. The fine silica bridges supporting the core are roughly 120 nm in width.

b) Core diameter 1.5 μm. The air holes are 0.62 μm in diameter

PCF: group-velocity dispersion

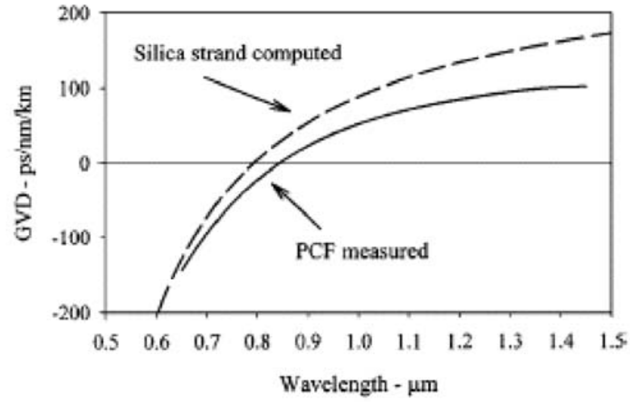

Fig. 3. Measured GVD from the fiber structure shown in Fig. 1(b) (solid line) and the corresponding computed curve for an isolated silica fiber (dashed line).

J.C. Knight et al., IEEE
PTL 12, 807 (2000)

PCF: group-velocity dispersion

Fiber number	Pitch (µm)	Air hole size (µm)	Core size (µm)	Measured GVD-zero wavelength (nm)	GVD-zero wavelength of a silica rod (nm) of same size
1	-	-	1	565	552
2	0.8	0.4	1.25	700	600
3	1.0	0.62	1.45	660	639
4	1.58	1.24	2.0	740	717
5	1.85	1.1	2.6	840	793

J.C. Knight et al., IEEE
PTL 12, 807 (2000)

Fiber Dispersion

The fiber is characterized by two 'zero dispersion wavelengths'

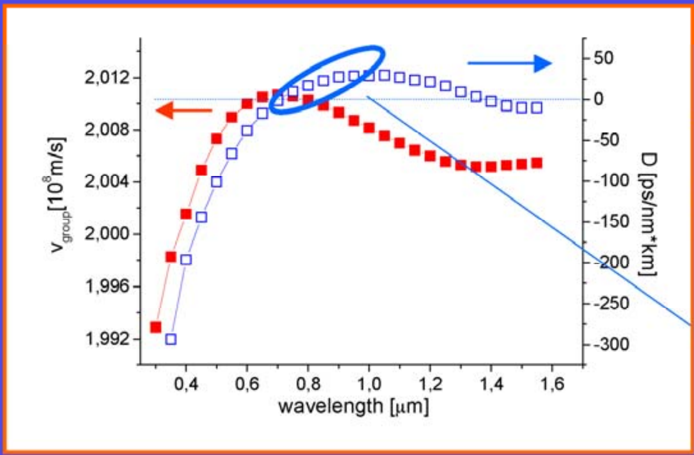

The holey fiber dispersion behaviour has been simulated by Pirelli Labs group by using a commercial BPM software (Rsoft)

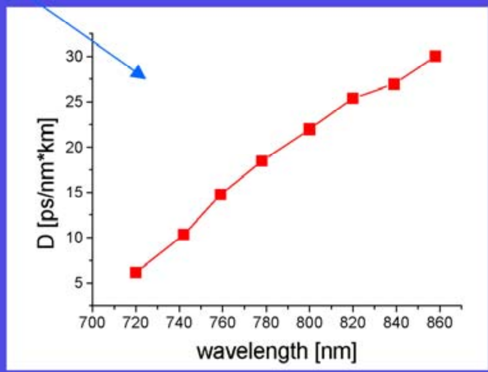

We checked the simulation by measuring experimentally the fiber GVD around 800 nm
We estimate the first zero dispersion wavelength at **λ = 704 nm**

PCF: birefringence

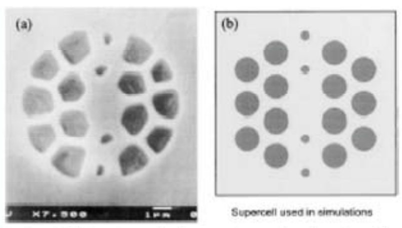

Fig. 1. (a) Scanning-electron micrograph, showing detail of the cross section of the core region of the fiber used in the experiment. The central silica region, surrounded by airholes, acts as the fiber core. (b) Idealized structure used in the numerical modeling.

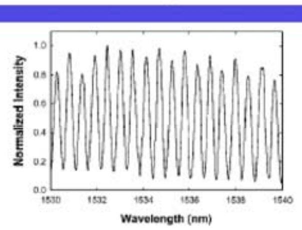

Fig. 3. Typical plot of the signal transmitted through a polarizer placed at the end of the fiber. The fiber length was 860 mm. Note that the overall transmitted intensity is constant.

A. Ortigosa-Blanch et al., Opt. Lett. 25, 1325 (2000)

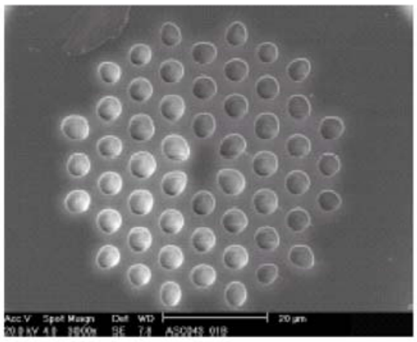

Fig. 1. SEM image of the cross-section of the fibre.

Temperature independent highly birefringent photonic crystal fibre

Andrew Michie, John Canning, Katja Lyytikäinen, Mattias Åslund, and Justin Digweed

Optical Fibre Technology Centre, University of Sydney & Australian Photonics Cooperative Research Centre, Eveleigh1430 NSW Australia
a.michie@oftc.usyd.edu.au
http://www.oftc.usyd.edu.au

Abstract: A highly birefringent photonic crystal fibre has been characterised as a function of temperature. The modal birefringence has been found to be independent of temperature from –25 to 800 °C.

Propagation losses

Propagating power: $P(z) = P_o \exp(-\alpha_o z)$

Usually the attenuation constant is given in dB/km:

$\alpha(\text{dB/km}) = 4.34\ \alpha_o\ (\text{km}^{-1})$

Standard silica fiber: α = 0.15 dB/km at 1550 nm

Silica-core PCF: α = 20-50 dB/km

Air-core PCF: in principle, α could be smaller than for standard silica fibers

Polymeric PCF

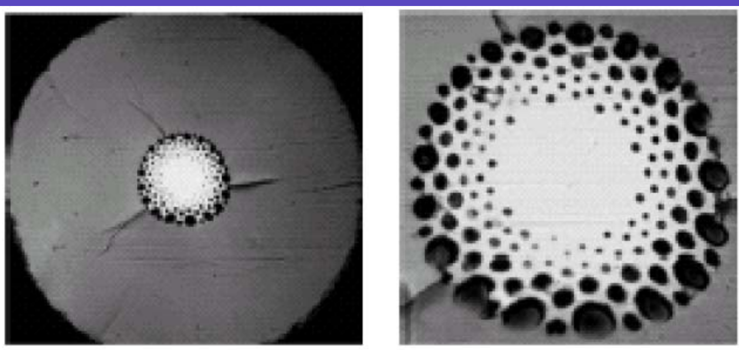

Fig. 1 *Optical micrographs of multimode graded-index microstructured polymer optical fibre (GImPOF) with core diameter of 135 µm and outer diameter of 520 µm*

Polymeric fibers: the preform is a PMMA rod with 216 holes of varying diameter. MA van Eijkelenborg et al., Electron. Lett. 40, 592 (2004)

Polymeric PCF

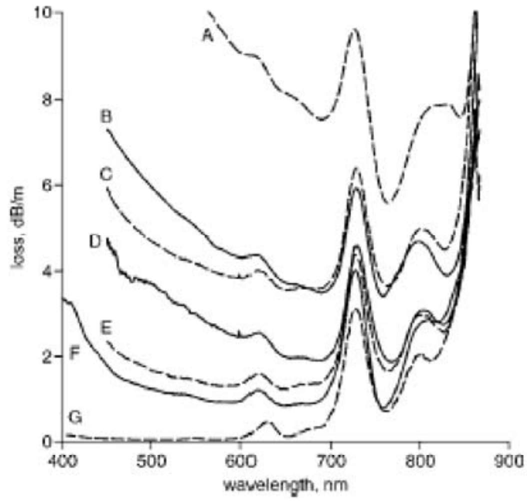

Fig. 2 *Measured transmission losses of graded-index polymer optical fibres labelled A–F as fabricated under conditions listed in Table 1*

-Polymeric fibers: The lowest loss: 0.80 dB/m at 760 nm.

-Short-distance optical communications: 2.4 Gbit/s can be transmitted at 653 nm over a distance of 100 m.

High-power large-mode-area PCF laser

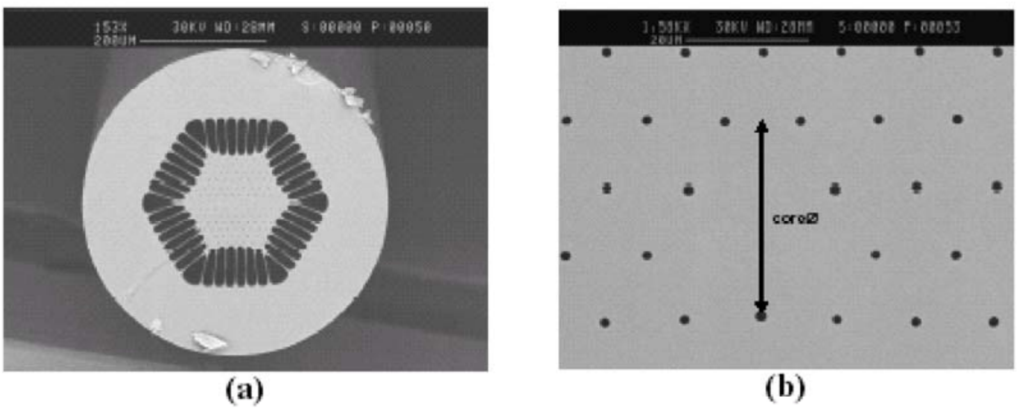

Fig. 1. Scanning electron microscope images of the air-clad ytterbium-doped large-mode-area fiber; (b) close-up of core region

Core diameter 28 μm, d = 2 μm, d/Λ = 0.18

Ytterbium-doped double-clad fiber.

J. Limpert et al., Opt. Express 11, 818 (2003)

High-power large-mode-area PCF laser

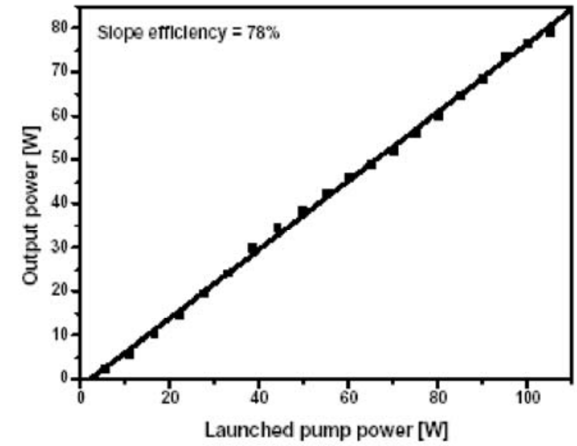

Fig. 3. Laser characteristics of the high power air-clad microstructure ytterbium-doped large-mode-area fiber

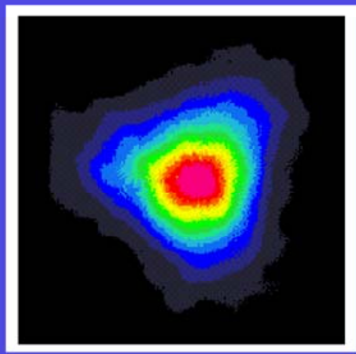

Y-doped fiber length: 2.3 m, 976-nm pump, threshold pump power 0.75 W, nearly diffraction limited output at 1070 nm.

J. Limpert et al., Opt. Express 11, 818 (2003)

Nonlinear properties of silica-core PCFs

Extreme nonlinear characteristics:

- Very large interaction length (L of the order of meters)
- Effective area A_{eff} = 2 μm^2 (standard fiber A_{eff} = 80 μm^2 @ 1.5 μm)

$$\frac{\partial A}{\partial z} + \beta_1 \frac{\partial A}{\partial t} + \beta_2 \frac{\partial^2 A}{\partial t^2} + \frac{\alpha}{2} A = i\gamma |A|^2 A$$

Nonlinear coefficient $\gamma = \frac{2\pi n_2}{\lambda A_{eff}}$ ⇨ 40 times larger than in standard fibers

Typical Nonlinear PCF (Crystal-fibre product)

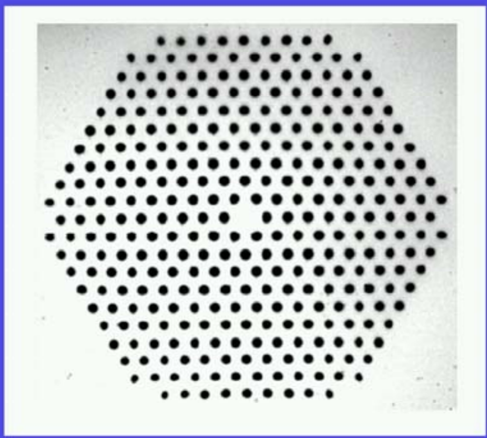

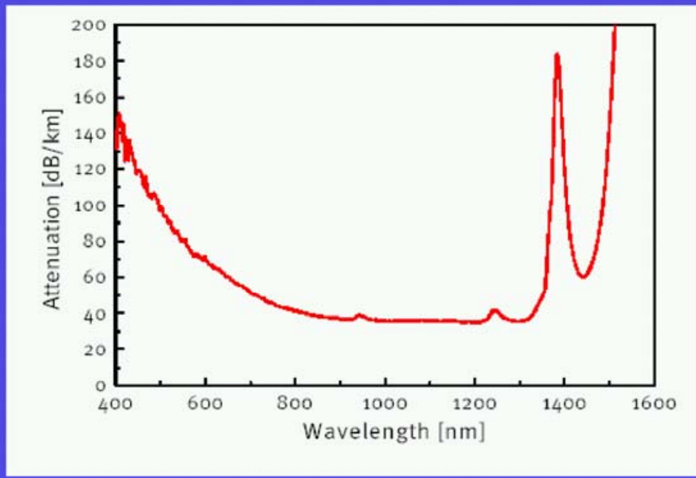

Short Zero dispersion wavelength:	750 ± 15 nm
Long Zero dispersion wavelength:	1260 ± 20 nm
Attenuation @ 780 nm:	<0.05 dB/m
Cut-off wavelength:	<650 nm
Mode field diameter @ 780 nm:	1.6 ± 0.3 µm
Numerical aperture @ 780 nm:	0.38 ± 0.05
Nonlinear coefficient @ 780 nm:	~ 95 $(Wkm)^{-1}$
Birefringence @ 780 nm	$>3\cdot10^{-4}$

Experimental set-up

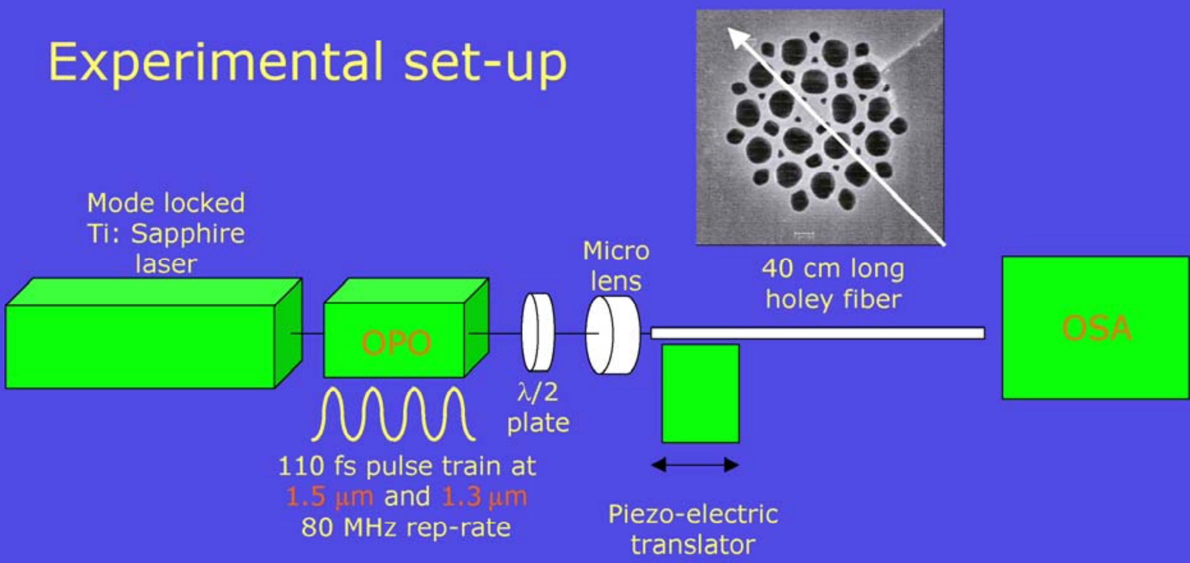

Laser pulses are linearly polarized along one principal axis of the birefringent holey fiber

Super-continuum generation

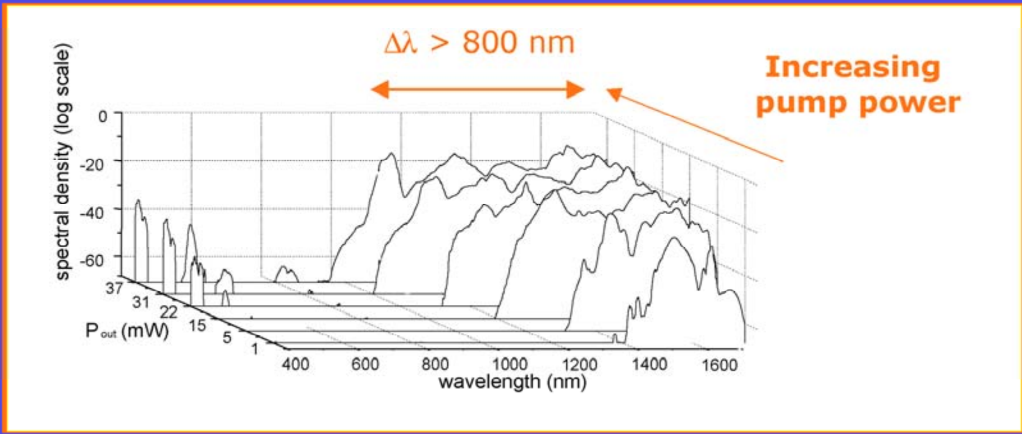

•Interplay between self-phase modulation (SPM), stimulated Raman scattering (SRS), four-wave mixing (FWM)

•Possible applications: multiwavelength light source suitable for WDM optical communications, high-speed spectroscopy over wide wavelength range, high-precision optical metrology, ...

Tartara et al. Opt. Comm., 215, 191, 2003

Optical frequency metrology

Techniques using femtosecond-laser frequency combs can count optical frequencies of hundreds of Terahertz. Extremely narrow optical resonances in cold atoms can be measured with high resolution. A laser locked to a narrow resonance could serve as an highly stable oscillator for an all-optical atomic clock.

Optical frequency metrology

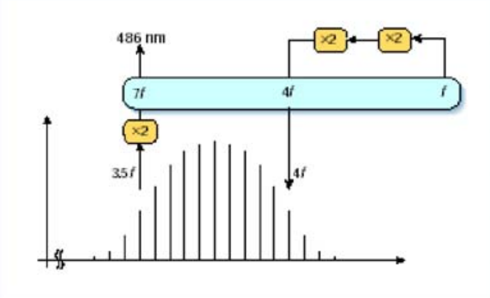

Figure 2 The first direct radio frequency–optical frequency conversion using a femtosecond laser. As explained in the text, the optical frequency interval divider (blue box) fixes the frequency ratios to precisely $7f:4f:f$. With the frequency quadrupling stage, which was already used to measure other optical transition frequencies relative to a He–Ne reference, the frequency comb fixes the interval $4f - 3.5f = 0.5f$ and therefore f and any other frequency in the set-up.

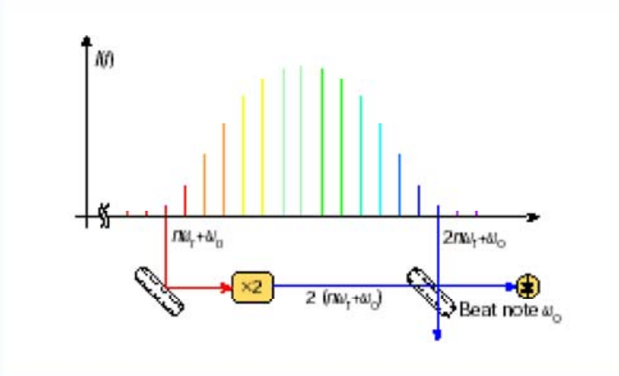

Figure 3 The principle of the single-laser optical synthesizer. A mode with the mode number n at the red wing of the comb and whose frequency is given according to equation (2) by $\omega_n = n\omega_r + \omega_0$ is frequency doubled in a nonlinear crystal. If the frequency comb covers a full optical octave, a mode with the number $2n$ should oscillate simultaneously at $\omega_{2n} = 2n\omega_r + \omega_0$. The beat note between the frequency-doubled mode and the mode at $2n$ yields the offset frequency $2(n\omega_r + \omega_0) - (2n\omega_r + \omega_0) = \omega_0$.

Optical frequency metrology

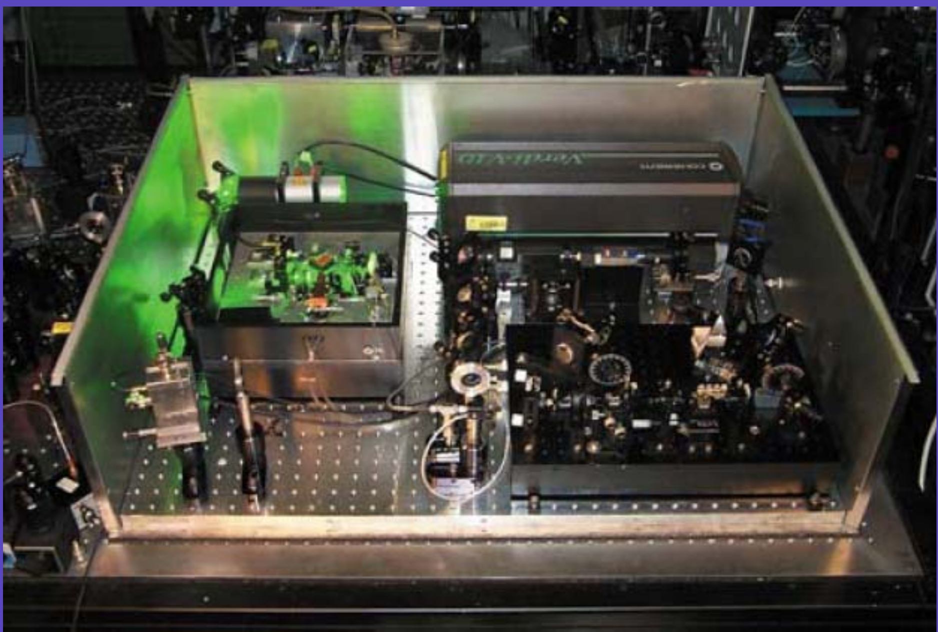

Hollow-core PCF: transmission window

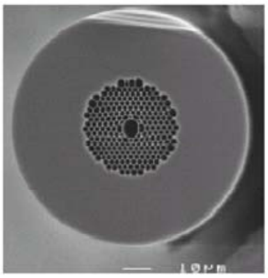

Fig. 1. Scanning electron micrograph of the 850 nm air-core fiber used in this work. The outer diameter of the fiber is 85 µm.

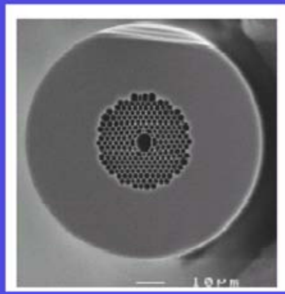

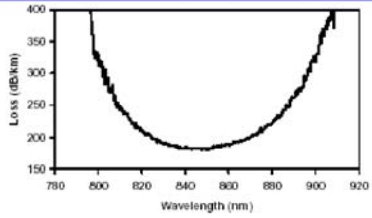

Fig. 2. Attenuation recorded using a cutback measurement on 56 m of fiber. Outside of this spectral window, no low-loss wavelength bands were observed.

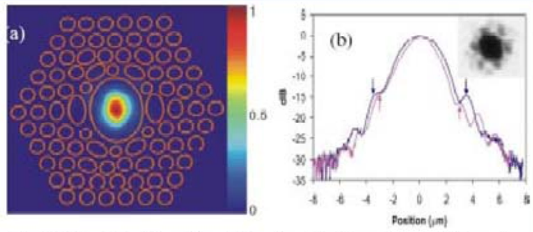

Fig. 3. (a) Near-field pattern of the guided mode, recorded at a wavelength of 848 nm after transmission through 60 m of fiber (linear scale). The location of the first few rings of air holes are represented schematically as the orange outlines. (b) Line plots through the two axes of the elliptical core, in a logarithmic scale, with arrows indicating the positions of the core wall. The inset shows the far-field pattern, as recorded on infrared photographic film.

G. Bouwmans et al., Opt. Express 11, 1613 (2003)

Air-core photonic crystal fibers

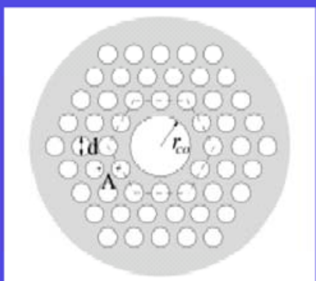

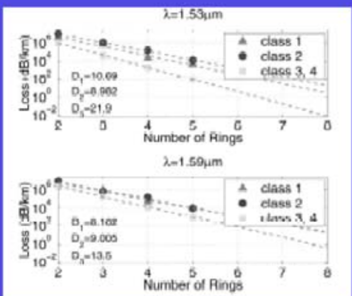

Y. Xu and A. Yariv, Opt. Lett. 28, 1885 (2003)

Hollow-core PCF: losses

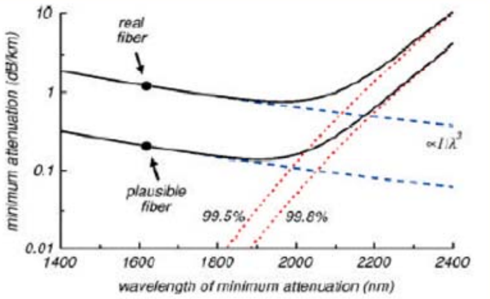

Fig. 5. Modelled bulk (dotted red lines) and surface (broken blue lines) contributions to the net (solid lines) minimum attenuation of 19-cell HC-PCFs, based on actual and plausible attenuation values at 1620 nm wavelength under the assumptions described in the text. Corresponding values of f_b are marked on the bulk attenuation curves.

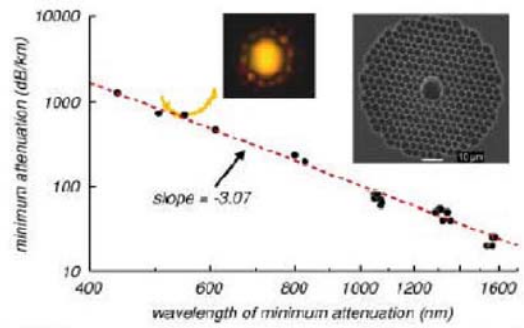

Fig. 4. (solid orange curve) The low-loss part of the measured attenuation spectrum of a 7-cell HC-PCF, with a minimum of 700 dB/km at λ_c = 550 nm. (left inset) Measured near-field pattern at the output of this fibre at 550 nm. (points) The minimum attenuation of similar HC-PCFs with various transverse scales, versus the wavelength λ_c of minimum attenuation. (broken red line) A straight-line fit to the points, having a slope of −3.07. (right inset) SEM of a representative of these HC-PCFs, with $\lambda_c \approx$ 1550 nm.

Scattering losses due to surface roughness

P.J. Roberts et al., Opt. Express 13, 236 (2005)

Hollow-core PCF: dispersion

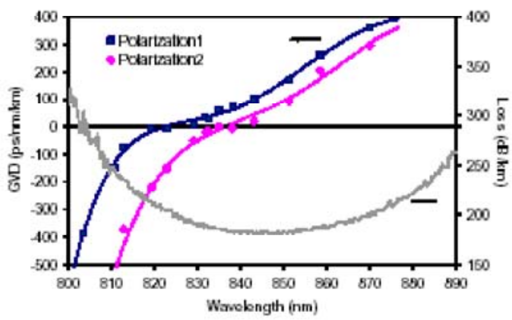

Fig. 7. Group velocity dispersion curves measured for the two polarization modes using the time-domain technique. Output pulse lengths were measured with an autocorrelator, and the sign of the dispersion was obtained from the low-coherence data. The attenuation curve is shown here for ease of reference.

THE GVD of the fundamental mode is low and anomalous over most of the transmission band, passing through zero towards the shorter-wavelength edge of the bandgap. The fiber presents a core ellipticity of 10-15%. This causes a splitting between the fundamental polarization modes of the order of a few times 10^{-4}.

Hollow-core PCF: attenuation and dispersion

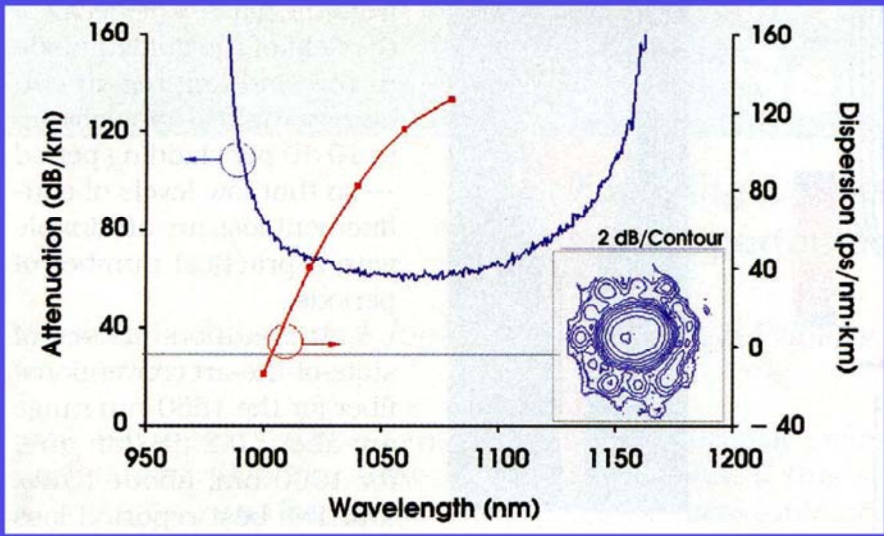

The group-velocity dispersion in hollow-core PCFs is dominated by waveguide dispersion. D passes through zero within the low-loss transmission window, enabling the design of fibers with normal, near-zero or anomalous dispersion at any given wavelength. [H. Sabert and J. Knight, Photonics Spectra, August 2003]

Hollow-core PCF: delivery of distortion-free fs pulses

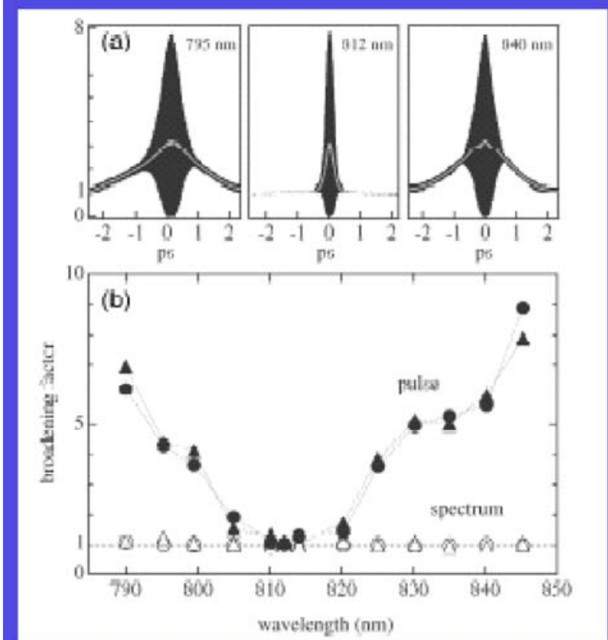

λ_{ZD}= 812 nm, L = 1.5 m, 50% loss

9-μm-diameter core surrounded by a 40-μm-diameter microstructured cladding

W- Goebel et al., Opt. Lett. 29, 1285 (2004)

Fig. 2. Pulse propagation through the hollow-core fiber. (a) Autocorrelation measurements of output pulses at three different wavelengths (250-mW average output power). The interferometric autocorrelations are shown by the black traces, and the intensity autocorrelations are shown by the light curves. (b) Relative broadening of pulse width (filled shapes) and spectral width (open shapes) compared with the corresponding input pulse (170–290 fs). The dashed line indicates 100%. The widths are plotted for average output powers of 2 mW (circles) and 250 mW (triangles). No prechirp was used.

Hollow-core PCF: applications

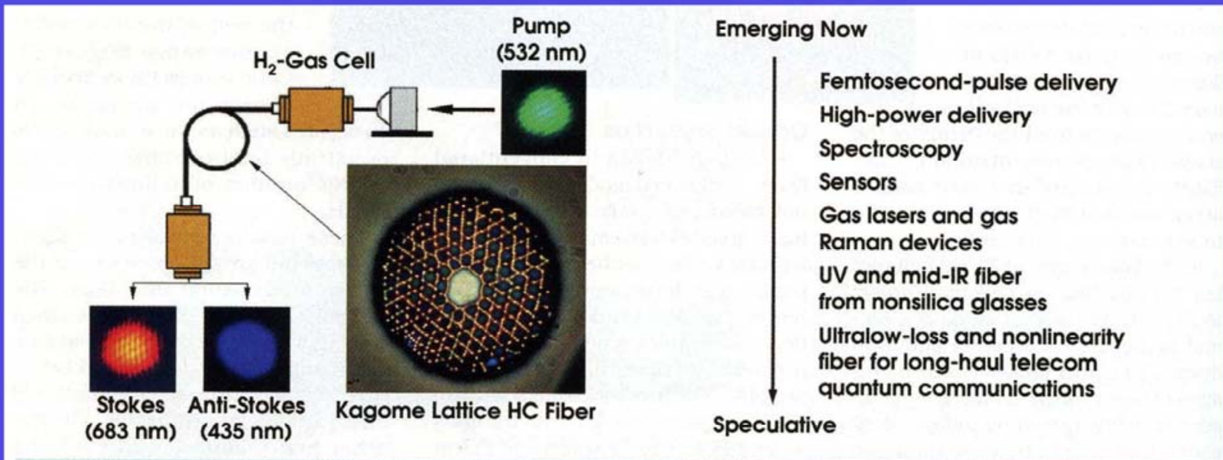

Figure 4. *Hollow-core fiber allows an increase in the interaction volume between an optical mode and gases or liquids almost limitlessly, reducing the threshold for nonlinear interactions to raising the sensitivity of spectroscopic experiments. In this case, the threshold power for the generation of stimulated Raman radiation in H_2 gas is reduced by more than 1000 times when compared with conventional gas cells.*

H. Sabert and J. Knight, Photonics Spectra, August 2003

Conclusions

- Microstructured fibers can outperform conventional optical fibers in several ways: the single-mode behavior can cover a wider wavelength interval, the single-mode area can be much larger (or much smaller), the dispersion properties can be tailored in a variety of ways, high birefringence is easily created, ...

- MFs may show new properties, such as propagation in an air-core

- Large number of applications, perhaps many are yet to be discovered